Electronic Supplementary Information (ESI) for

(*R*)- and (*S*)-$[C_8H_{10}NO_3]_2[NbOF_5]$: Noncentrosymmetric niobium oxyfluorides with large optical anisotropy

Jihyeon Moon and Kang Min Ok*

Department of Chemistry, Sogang University, 35 Baekbeom-ro, Mapo-gu, Seoul 04107, Korea

*E-mail: kmok@sogang.ac.kr

Table of contents

Single crystal X-ray diffraction. Colorless rod-shaped crystals of (*R*)-Nb (0.099 mm × 0.127 mm × 0.314 mm) and (*S*)-Nb (0.084 mm × 0.146 mm × 0.255 mm) were selected to collect single crystal X-ray diffraction (SC-XRD) data. SC-XRD was conducted with a Bruker D8 QUEST diffractometer using a graphite-monochromated Mo Kα (λ = 0.71073 Å) radiation and a PHOTON-II CPAD detector at 100 K for **(*R*)-Nb** and **(*S*)-Nb**. Through the SAINT program, the collected data were integrated. The structure solution and refinement of the title compounds were conducted via SHELXS-2013[1] and SHELXL-2015,[2] respectively, implemented in the program WinGX-2014.[3]

Table S1. Crystallographic data for (*R*)-Nb and (*S*)-Nb

	(*R*)-Nb	**(*S*)-Nb**
formula	$(C_8H_{10}NO_3)_2NbOF_5$	
fw	540.25	540.25
space group	$P2_12_12$	$P2_12_12$
a (Å)	13.4517(5)	13.4489(7)
b (Å)	7.4357(3)	7.4392(4)
c (Å)	10.2751(4)	10.2681(5)
α (°)	90	90
β (°)	90	90
γ (°)	90	90
V (Å^3)	1027.74(7)	1027.31(9)
Z	2	2
T (K)	100(2)	100(2)
λ (Å)	0.71073	0.71073
ρ_{calcd} (g/cm^3)	1.746	1.747
$R(F_o)^a$	0.0166	0.0129
$R_w(F_o^2)^b$	0.0169	0.013
Flack x	-0.039(10)	-0.023(6)

$^aR(F) = \Sigma \, ||F_o| - |F_c|| \, / \, \Sigma \, |F_o|$.

$^bR_w(F_o^2) = [\Sigma w(F_o^2 - F_c^2)^2 \, / \, \Sigma w(F_o^2)^2]^{1/2}$.

Table S2. Selected distances (Å) for (*R*)-Nb

Nb(1)-F(1)	2.0285(12)
Nb(1)-F(2)	1.9521(11)
Nb(1)-F(3)	1.8405(13)
C(1)-C(2)	1.513(3)
C(1)-C(8)	1.529(3)
C(1)-N(1)	1.498(2)
C(2)-C(3)	1.394(3)
C(2)-C(7)	1.392(3)
C(3)-C(4)	1.388(3)
C(4)-C(5)	1.391(3)
C(5)-C(6)	1.392(3)
C(5)-O(1)	1.371(2)
C(6)-C(7)	1.397(3)
C(8)-O(2)	1.210(2)
C(8)-O(3)	1.310(3)

Table S3. Hydrogen bond distances (Å) for (*R*)-Nb

D-H...A	d(D...A)	D-H...A	d(D...A)
N(1)-H(1A)...O(2)#2	2.743(2)	N(1)-H(1C)...O(1)#5	2.868(2)
N(1)-H(1A)...F(2)#3	2.949(2)	O(1)-H(1O)...F(2)#6	2.7178(19)
N(1)-H(1B)...O(4)#4	2.866(2)	O(3)-H(3O)...F(1)	2.5326(19)

Symmetry transformations used to generate equivalent atoms:

#1 -x+1,-y,z #2 -x+3/2,y+1/2,-z #3 -x+1,-y+1,z #4 x+1/2,-y+1/2,-z

#5 -x+3/2,y+1/2,-z+1 #6 -x+1,-y+1,z+1

Table S4. Selected distances (Å) for (*S*)-Nb

Nb(1)-F(1)	2.0271(10)
Nb(1)-F(2)	1.9506(9)
Nb(1)-F(3)	1.8433(11)
C(1)-C(2)	1.512(2)
C(1)-C(8)	1.528(3)
C(1)-N(1)	1.496(2)
C(2)-C(3)	1.395(2)
C(2)-C(7)	1.392(2)
C(3)-C(4)	1.389(2)
C(4)-C(5)	1.390(2)
C(5)-C(6)	1.392(2)
C(5)-O(1)	1.3713(2)
C(6)-C(7)	1.395(2)
C(8)-O(2)	1.2101(18)
C(8)-O(3)	1.312(2)

Table S5. Hydrogen bond distances (Å) for (*S*)-Nb

D-H...A	d(D...A)	D-H...A	d(D...A)
N(1)-H(1A)...O(2)#3	2.7434(18)	N(1)-H(1C)...O(4)#5	2.8682(18)
N(1)-H(1A)...F(2)#2	2.9452(17)	O(1)-H(1O)...F(2)#6	2.7142(16)
N(1)-H(1B)...O(1)#4	2.8662(19)	O(3)-H(3O)...F(1)	2.5312(16)

Symmetry transformations used to generate equivalent atoms:

#1 -x+1,-y+2,z #2 -x+1,-y+1,z #3 -x+1/2,y-1/2,-z+2 #4 -x+1/2,y-1/2,-z+1

#5 x-1/2,-y+3/2,-z+2 #6 -x+1,-y+1,z-1

Single crystal growth. To obtain large-sized crystals, additional experiments were conducted by controlling the amount of reagents. 12.0 mmol portion of Nb_2O_5 was dissolved in 6 mL of a 48 % aqueous HF solution and the mixture was place in and 18mL Teflon-lined autoclave. After closing, the autoclave was heated at 100 °C for 7 h to obtain a clear Nb_2O_5/HF solution and prepare two Nb_2O_5/HF solution through the same step. After cooling to room temperature, all the prepared Nb_2O_5/HF solutions were put into the 100 mL polymethylpentene beakers, which have chemical resistance to HF. Afterwards, 4-Hydroxy-D-(-)-2-phenylglycine (96.0 mmol, 16.047g) was added to the beakers with 48 mL of distilled water and stirred for 20 min. The reaction mixtures were evaporated at room temperature. Transparent crystals were grown at the interface or bottom of the mixtures as the solvent evaporates. Millimeter- to centimeter-sized crystals were grown in 20 days.

Figure S1. Photos of crystal growth processes

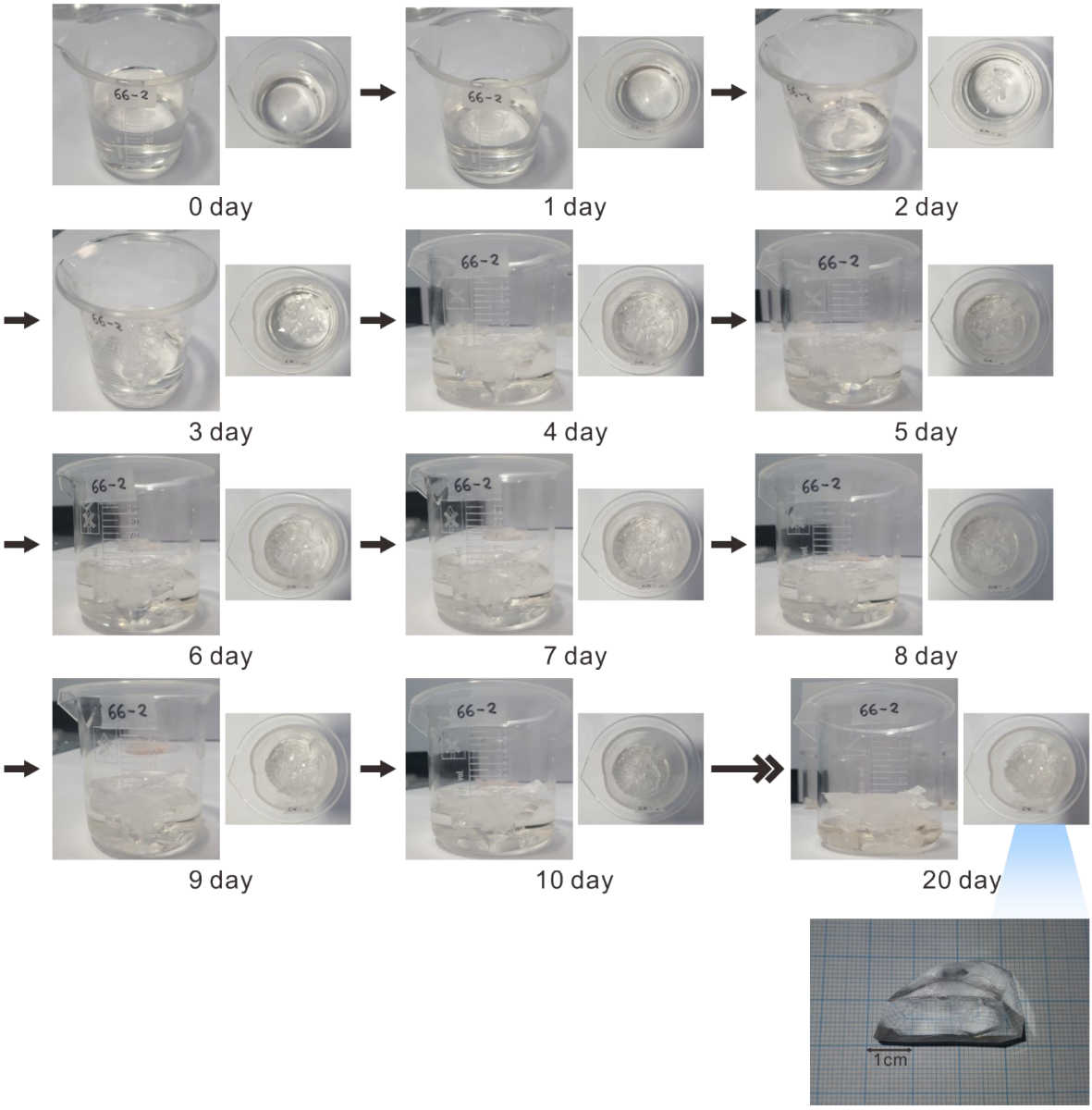

Figure S2. Distances (Å) of adjacent (*R*)-HPG cations in a unit cell

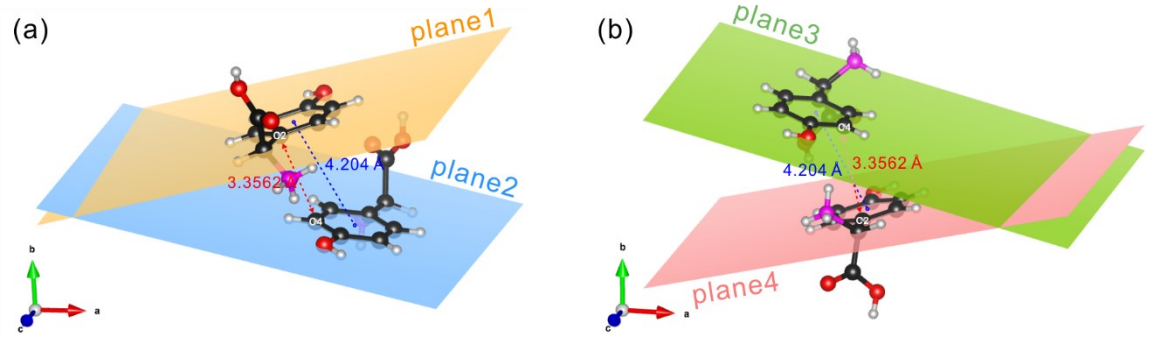

Powder X-ray diffraction (PXRD). PXRD were conducted by using a Rigaku MiniFlex 600 using Cu Kα (λ = 1.5406 Å) radiation. Polycrystalline samples of the title compounds were loaded on sample holders and scanned in the 2θ range of 5–70° with a step size of 0.02° for 0.1 s.

Figure S3. Experimental and calculated powder X-ray diffraction patterns of (*R*)-Nb and (*S*)-Nb

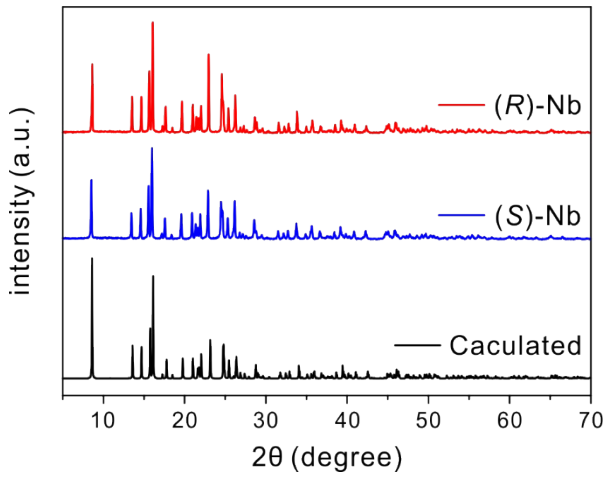

Elemental Analyses (EA). EA were conducted through a Thermo Flash 2000 Flash EA1112 analyzer. Polycrystalline samples were mounted on an Sn capsule and entered Dynamic Flash Combustion. The starting temperature is 1000 °C and the temperature at which the samples is oxidized is 1800 °C.

Table S6. EA data for (*R*)-Nb and (*S*)-Nb

Element	Calculated	Experimental	
		(*R*)-Nb	(*S*)-Nb
N	5.19	5.24	5.25
C	35.57	35.46	35.57
H	3.73	3.76	3.76
Totals	44.49	44.46	44.58

Figure S4. EA data for (*R*)-Nb and (*S*)-Nb

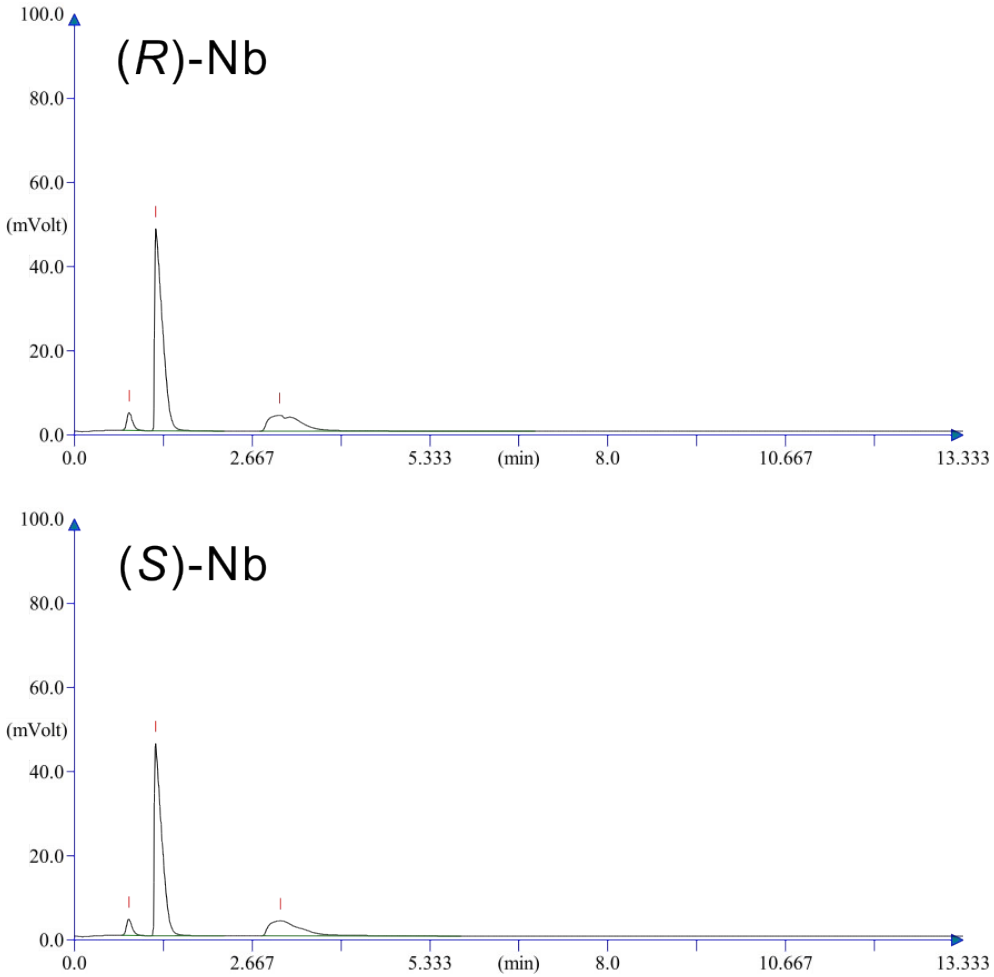

Energy dispersive analysis by X-ray (EDX). EDX was conducted by a JSM-7100F Thermal field emission electron microscope with lens type ZrO/W Schottky field emission gun. Well-ground solid samples of the title compounds were attached on carbon tape and coated by Pt before the measurements.

Table S7. SEM-EDX data for (*R*)-Nb and (*S*)-Nb

	(*R*)-Nb		**(*S*)-Nb**	
Element	Wt %	Atomic %	Wt %	Atomic %
C	46.07	58.82	47.04	59.42
N	6.81	7.46	6.46	6.99
O	17.43	16.71	16.99	16.12
F	18.86	15.23	19.9	15.9
Nb	10.83	1.79	9.61	1.57
Total	100		100	

Figure S5. SEM-EDX spectra for (*R*)-Nb and (*S*)-Nb

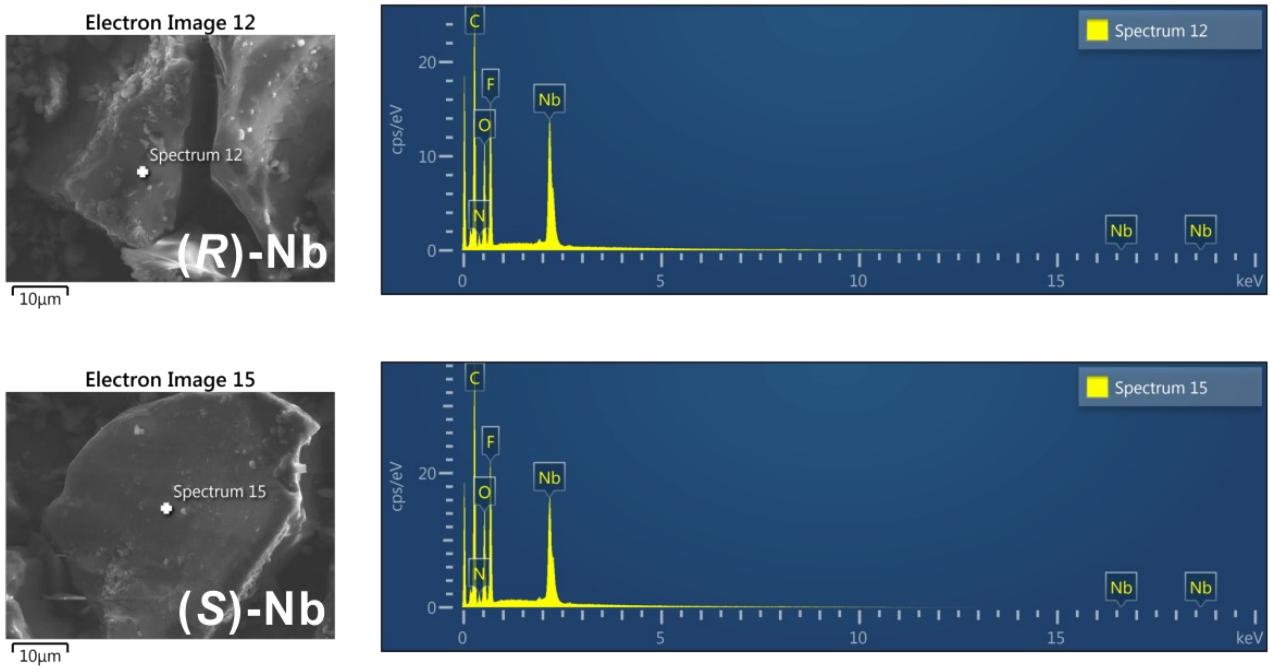

Infrared (IR) spectroscopy. FT-IR spectra were obtained by using a Thermo Scientific Nicolet iS50 FT-IR spectrometer with an attenuated total reflection (ATR) accessory in the range of 400–4000 cm^{-1}.

Figure S6. IR spectra for (*R*)-Nb and (*S*)-Nb

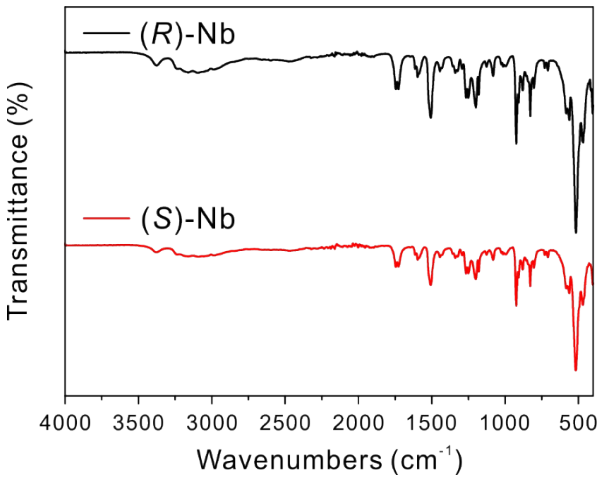

Ultraviolet-visible (UV-vis) diffuse-reflectance spectroscopy. UV-vis diffuse-reflectance spectra were measured by using a Lambda 1050 spectrophotometer in the range of 185–900 nm. The band gap energy was obtained by using the Kubelka-Munk function.

Figure S7. UV-vis spectra for (*R*)-Nb and (*S*)-Nb

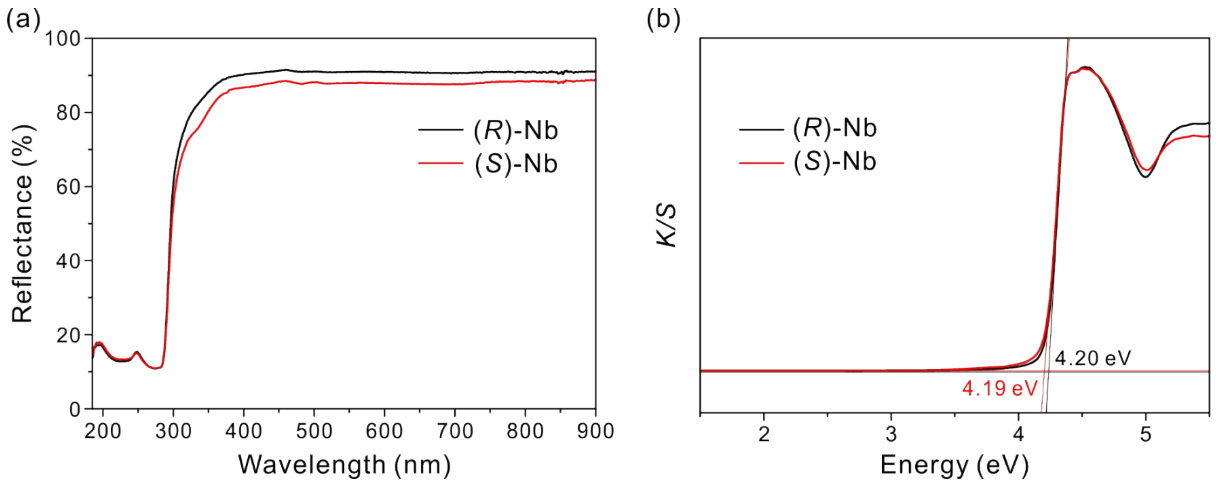

Thermogravimetric analyses (TGA). TGA were conducted by using a SCINCO TGA-N 1000 thermal analyzer. The ground samples of the title compounds were put in alumina crucibles and load on Pt crucibles. The samples were heated from 25 °C to 900 °C at a rate of 10 °C min^{-1} under flowing air.

Figure S8. TGA diagrams and PXRD patterns after heating at different temperatures for (*R*)-Nb and (*S*)-Nb

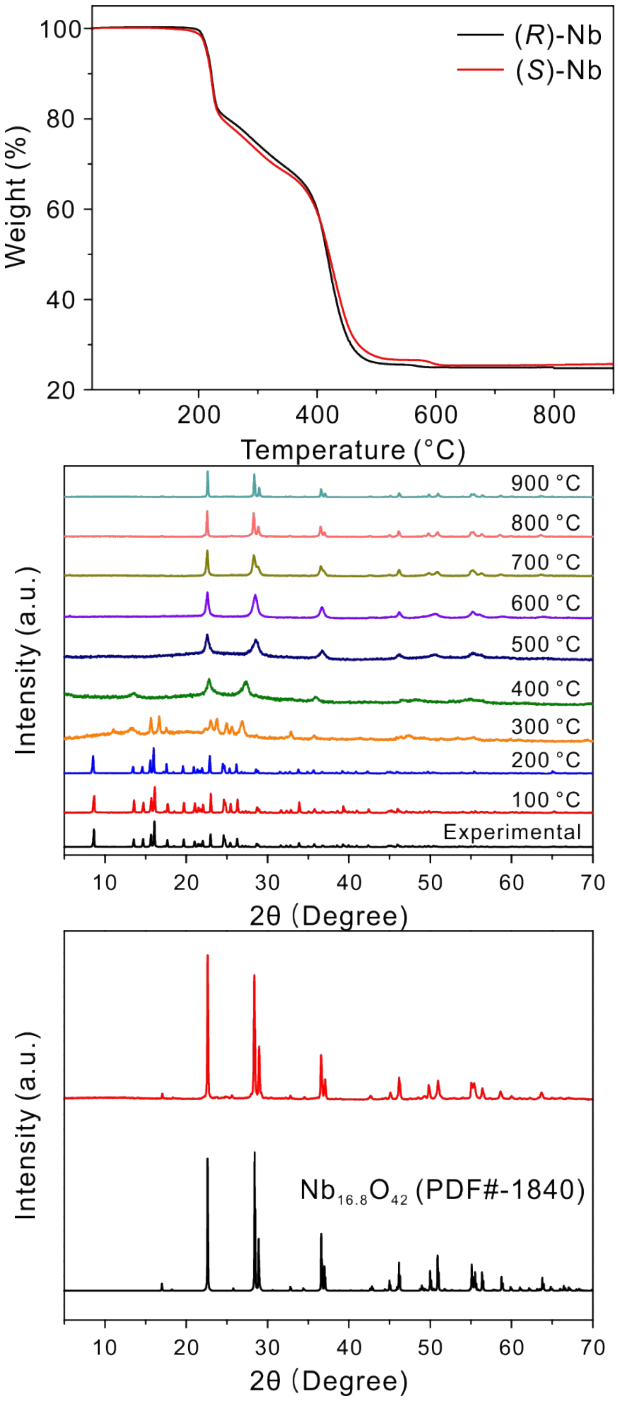

Figure S9. PXRD patterns of the original and recrystallized samples from water

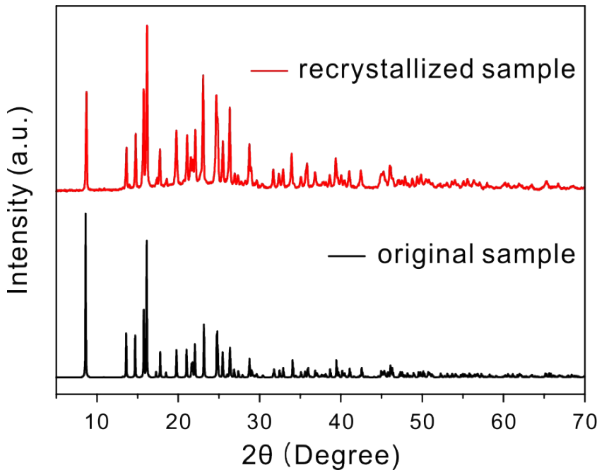

Powder second harmonic generation (SHG) measurements. Powder SHG measurements were executed by using the well-ground and sieved polycrystalline samples into the diverse particle size ranges: 0–20, 20–45, 45–63, 63–75, 75–90, 90–125, 125–150, 150–200, and 200–250 μm. Each samples in specific capillary tubes are irradiated by DAWA Q-switched Nd:YAG laser with 1064 nm radiation. The SHG light (532 nm) was collected to a Hamamatsu photomultiplier tube and monitored by a Tektronix TDS-2012C oscilloscope.

Figure S10. Particle size dependent SHG intensity curves for (*R*)-Nb and (*S*)-Nb

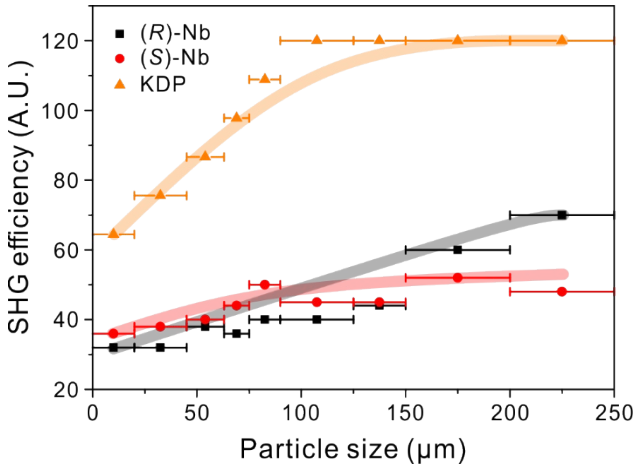

Table S8. Calculated dipole moments for (*R*)-Nb (D = Debye)

		Dipole moment (D)		
Unit	Magnitude (D)	x	y	z
$Nb(1)(O/F)_2F_4$	2.46	0	0	-2.46
$Nb(2)(O/F)_2F_4$	2.46	0	0	2.46
$Nb(3)(O/F)_2F_4$	2.46	0	0	-2.46
$Nb(4)(O/F)_2F_4$	2.46	0	0	2.46
Net	0	0	0	0

Figure S11. Net moments of $[Nb(O/F)_2F_4]^{2-}$ polyhedra in a unit cell for (*R*)-Nb

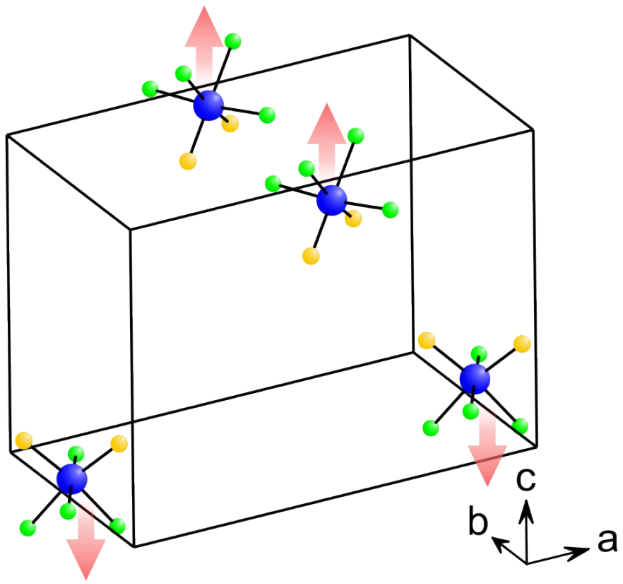

Density functional theory (DFT) calculations. DFT calculations were performed to obtain the electronic structures based on the Quantum Espresso package.[4] For structural optimization, crystal data models from SC-XRD analysis were used. The ultrasoft pseudopotential with Perdew–Burke–Ernzerhof (PBE) functional and the scalar relativistic effect about constituent elements (C, H, N, O, F and Nb) were downloaded from the Quantum Espresso website.[5] For the title compounds, the cutoff energies for the wave function and the charge density were set to 49.146 and 326.261 Ry, respectively. The self-consistent function (SCF) convergence criterion was set to less than 10^{-6} Ry. Also, SCF and band structure were computed in 2 × 4 × 3 k-point grids of the Brillouin zone.

Figure S12. Band structures for (a) (*R*)-Nb and (b) (*S*)-Nb. Arrows display the optical transition from the valence band maximum to the conduction band minimum.

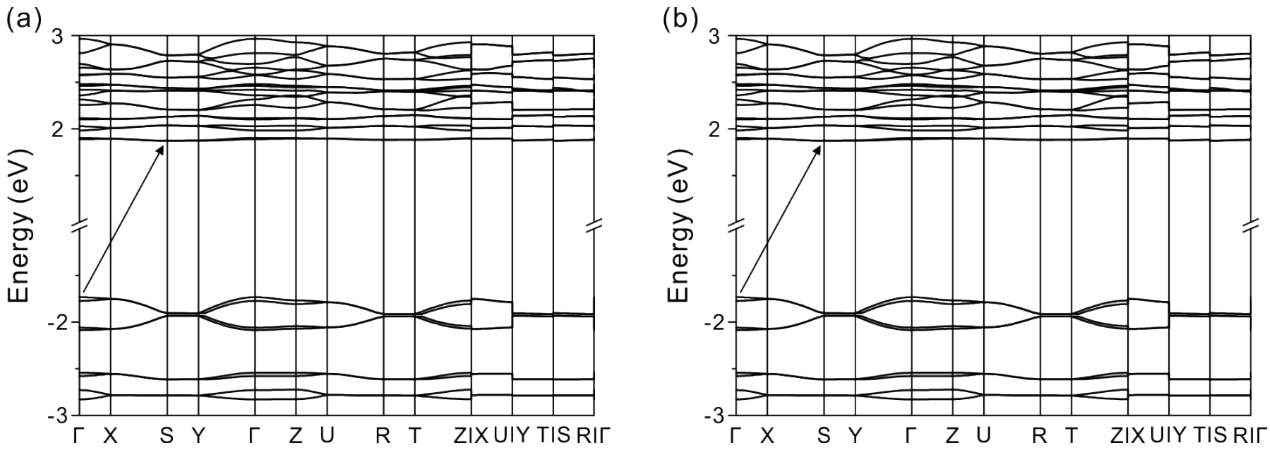

Birefringence. The immersion technique[6] was conducted to observe birefringence. Two hand-polishing (200) and (201) single crystals which each plane is confirmed by PXRD pattern are used by gem refractometer and gem refractometer liquid oil. The refractive indices of single crystals are observed up to three decimal places on the scale graduation by rotating the single crystals from 0° to 360°. In order to calculate the refractive index, a norm-conserving pseudopotential method was used. The calculation was conducted by YAMBO[7-10] with correction of band gap by using scissor operator.

Figure S13. Photos of hand-polishing crystals on glass hemicylinders for (a) (200) and (b) (201) crystals.

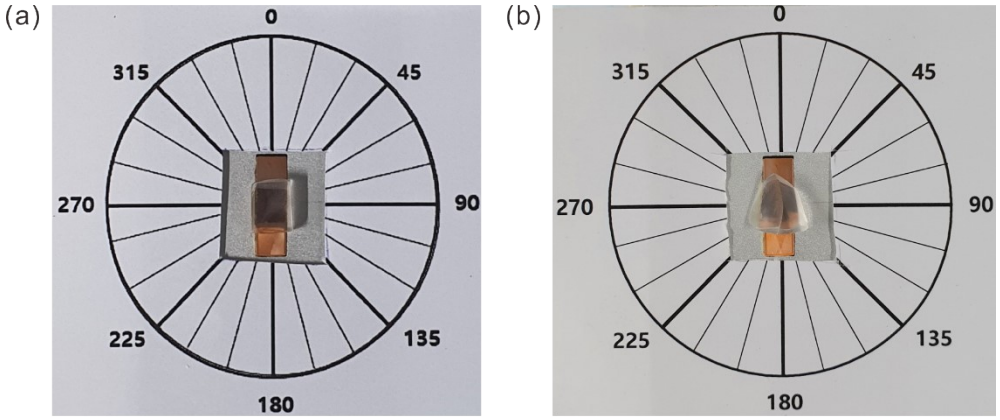

Table S9. Refractive index measured by rotating the (200) crystal from 0° to 360°.

Rotation angle	0°	15°	30°	45°	60°	75°	90°	105°	120°	135°	150°	165°
n	1.570	1.565	1.570	1.570	1.571	1.569	1.531	1.481	**1.452**	1.463	1.490	1.519
		1.622	1.644	**1.651**	1.621	1.583	1.574	1.560	1.554	1.559	1.561	1.560
Rotation angle	180°	195°	210°	225°	240°	255°	270°	285°	300°	315°	330°	345°
n	1.570	1.569	1.570	1.572	1.571	1.569	1.532	1.482	1.460	1.464	1.491	1.515
		1.621	1.643	1.651	1.630	1.591	1.570	1.560	1.560	1.556	1.560	1.564

Table S10. Refractive index measured by rotating the (201) crystal from 0° to 360°.

Rotation angle	0°	15°	30°	45°	60°	75°	90°	105°	120°	135°	150°	165°
n	1.520	1.520	1.518	1.489	1.473	**1.460**	1.468	1.471	1.481	1.488	1.505	1.515
	1.603	1.568	1.562	1.562	1.573	1.598	1.619	1.639	1.641	**1.650**	1.643	1.624
Rotation angle	180°	195°	210°	225°	240°	255°	270°	285°	300°	315°	330°	345°
n	1.528	1.518	1.50	1.494	1.471	1.486	1.471	1.478	1.485	1.472	1.509	1.513
	1.601	1.563	1.572	1.571	1.598	1.598	1.620	1.642	1.648	1.650	1.644	1.618

Figure S14. Calculated birefringence for (*S*)-Nb

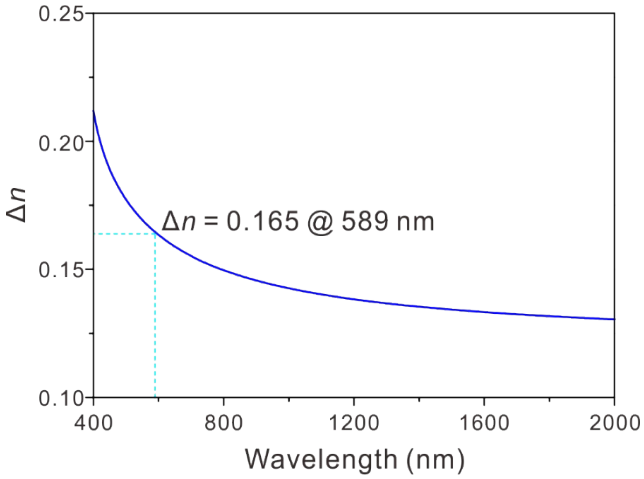

Figure S15. 2D Electron localization function maps of sliced planes in a unit cell of (*S*)-Nb.

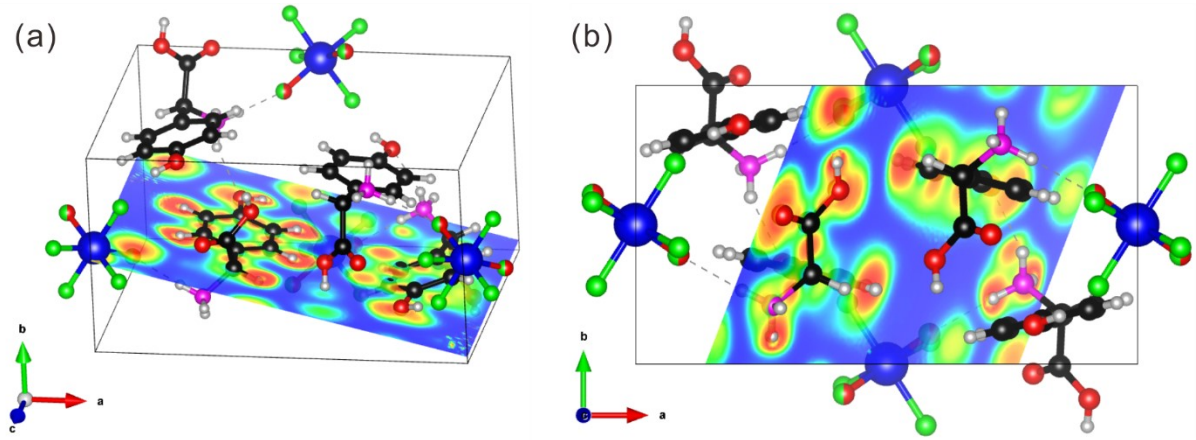

References

1. Sheldrick, G., SHELXS-2013/1, program for the solution of crystal structures. *Germany, University of Göttingen* **2013**.
2. Sheldrick, G. M., Crystal structure refinement with SHELXL. *Acta Crystallogr. Sect. C: Struct. Chem.* **2015,** *71*, 3-8.
3. Farrugia, L. J., WinGX and ORTEP for Windows: an update. *J. Appl. Crystallogr.* **2012,** *45*, 849-854.
4. Giannozzi, P.; Andreussi, O.; Brumme, T.; Bunau, O.; Nardelli, M. B.; Calandra, M.; Car, R.; Cavazzoni, C.; Ceresoli, D.; Cococcioni, M., Advanced capabilities for materials modelling with Quantum ESPRESSO. *J. Phys.: Condens. Matter* **2017,** *29*, 465901.
5. Rademaker, L., A Practical Introduction to Density Functional Theory. *arxiv: 2011.09888* **2020**.
6. Chen, C.; Wang, Y.; Xia, Y.; Wu, B.; Tang, D.; Wu, K.; Wenrong, Z.; Yu, L.; Mei, L., New development of nonlinear optical crystals for the ultraviolet region with molecular engineering approach. *J. Appl. Phys.* **1995,** *77*, 2268-2272.
7. Adragna, G.; Del Sole, R.; Marini, A., Ab initio calculation of the exchange-correlation kernel in extended systems. *Phys. Rev. B* **2003,** *68*, 165108.
8. Marini, A.; Del Sole, R.; Rubio, A., Bound excitons in time-dependent density-functional theory: optical and energy-loss spectra. *Phys. Rev. Lett.* **2003,** *91*, 256402.
9. Rohlfing, M.; Louie, S. G., Electron-hole excitations and optical spectra from first principles. *Phys. Rev. B* **2000,** *62*, 4927.
10. Sottile, F.; Olevano, V.; Reining, L., Parameter-free calculation of response functions in time-dependent density-functional theory. *Phys. Rev. Lett.* **2003,** *91*, 056402.